



American Society of  
Mechanical Engineers

**ASME Accepted Manuscript Repository**

**Institutional Repository Cover Sheet**

I Iacopo Rossi  
*First* *Last*

ASME Paper Title: Physics-Based Dynamic Models of Three SOFC/GT Emulator Test Rigs

Authors: Iacopo Rossi, Alberto Traverso, Martina Hohloch, Andreas Huber and David Tucker

ASME Journal Title: Journal of Engineering for Gas Turbines and Power (GTP)

Volume/Issue 140/5 Date of Publication (VOR\* Online) Dec 06,2017

ASME Digital Collection URL: <http://gasturbinespower.asmedigitalcollection.asme.org/article.aspx?articleid=2657490>

DOI: 10.1115/1.4038152

\*VOR (version of record)



# PHYSICS BASED DYNAMIC MODELS OF THREE SOFC/GT EMULATOR TEST-RIGS

**Iacopo Rossi**  
University of Genoa  
Department of Mechanical  
Engineering  
Via Montallegro, 1  
16145 Genova, Italy  
[iacopo.rossi@edu.unige.it](mailto:iacopo.rossi@edu.unige.it)

**Alberto Traverso**  
University of Genoa  
Department of Mechanical  
Engineering  
Via Montallegro, 1  
16145 Genova, Italy  
[alberto.traverso@unige.it](mailto:alberto.traverso@unige.it)

**Martina Hohloch**  
German Aerospace Center  
(DLR)  
Institute of Combustion Technology  
Pfaffenwaldring 38-40  
70569 Stuttgart, Germany  
[martina.hohloch@dlr.de](mailto:martina.hohloch@dlr.de)

**Andreas Huber**  
German Aerospace Center (DLR)  
Institute of Combustion Technology  
Pfaffenwaldring 38-40  
70569 Stuttgart, Germany  
[andreas.huber@dlr.de](mailto:andreas.huber@dlr.de)

**David Tucker**  
National Energy Technology Laboratory  
(NETL)  
U.S. Department of Energy  
3610 Collins Ferry Road  
26507 Morgantown, WV (USA)  
[david.tucker@netl.doe.gov](mailto:david.tucker@netl.doe.gov)

## ABSTRACT

This paper presents the development, implementation and validation of a simplified dynamic modeling approach to describe SOFC/GT hybrid systems in three real emulator test-rigs installed at University of Genoa (UNIGE, Italy), German Aerospace Center (DLR, Germany) and National Energy Technology Laboratory (NETL, USA), respectively. The proposed modeling approach is based on an experience-based simplification of the physical problem to reduce model computational efforts with minimal expense of accuracy. Traditional high fidelity dynamic modelling requires specialized skills and significant computational resources. This innovative approach, on the other hand, can be easily adapted to different plant configurations, predicting the most relevant dynamic phenomena with a reduced number of states: such a feature will allow, in the near future, the model deployment for monitoring purposes or advanced control scheme applications (e.g. model predictive control). The three target systems are briefly introduced and dynamic situations analyzed for model tuning, first, and validation, then. Relevance is given to peculiar transients where the model shows its reliability and its weakness. Assumptions introduced during model definition for the three different test-rigs are discussed and compared. The model captured significant dynamic behavior in all analyzed systems (in particular those regarding the GT) and showed influence of signal noise on some of the SOFC computed outputs.

## INTRODUCTION

The technology of Solid Oxide Fuel Cell Gas Turbine (SOFC/GT) Hybrid Systems is widely expected to change the current situation and to boost the average energy efficiency of small size power system (<1 MW). After decades of research, through which some big Companies opted to quit the business, generating some doubts about real feasibility of hybrids, first results are now available. FuelCell Energy proposed its first Hybrid System (HS) configuration in natural gas distribution [1] and Mitsubishi Heavy Industries delivered its first prototype to Kyushu University [2-3], while LG Fuel Cell System is working on development and testing of its sub-MW system. Moreover, General Electric entered the business again proposing its Fuel Cell Combined Cycle configuration [4]. However, such systems are still far from cost-effectiveness. The high costs of an experimental facility based on a hybrid framework prevent many universities and research centers to conduct experimental campaigns. Only a few highly specialized research centers work on hybrid system emulator rigs, which do not include a real fuel cell stack [5-11]. As a consequence, many studies must be conducted only at simulation level [12-19].

Nevertheless, use of simulation tools is hard, for two main reasons: complexity of the environment and multi-disciplinary skills required. In addition, high fidelity simulation models usually require hundreds of states (i.e. plant information and measurements) to work. When this approach is translated on real plants, it is not possible to have access to all of the information as in a simulation environment. This prevents the portability of these simulation systems and limit the transfer of knowledge. To solve such issues, common also to neighbor fields such as combined cycle simulations, Gulen and Kim firstly proposed the opportunity to favorite the convenience of simulation tools [20]. Their goal was explicitly "to democratize" the field of simulation of energy systems proposing a

viable approach for simulation of GTCC. The goal of this work is to propose and validate a framework, which has the same viability philosophy, applied to SOFC/GT Hybrid Systems. The work proposed by Gulen and Kim was at first analyzed and discussed in [21] and it finally gave light to a model that performs fast start-up simulation [22]. A similar method for HS has been initially proposed [23] and further developed, discussed and validated. The goal is to obtain a simplified model able to dynamically describe a HS. This kind of models was originally defined to support plant operator decisions [20-22] and to enhance diagnostics of power plant [22]. The model here proposed has then the same targets, though also other applications can be outlined [24]. This paper presents the validation of the proposed approach through three emulator rigs.

## MODELLING FRAMEWORK

In analogy with what was proposed in [20] and discussed in [21-22], the presented approach must be considered a method for dynamic model development. The approach discussed in this section is an extension and development of [23]. It results in a sort of hybridization between a physics and a numerical model. The framework evolved and now it is structured around a series of terms that work as inputs to the model. Involved equations are derived from exact steady-state energy equations and considerations on physics constituting the problem. The dynamic behavior of the plant is handled by a series of time decay terms, i.e. a first order delay. Time constants governing the transient are derived from physical consideration and so they can be somehow determined beforehand [23]. In general, it is possible to define two major forcing terms for the model: the pressure ratio and the current. Temperature of the elements respond to Lumped Capacitance Method and so transients in temperature are governed by Eq.1.

$$T(t) = T_{in} + \Delta T(1 - e^{-t/\tau}) \quad (1)$$

In [23] load-dependent time constants were introduced to better capture the dynamics of the system. Considering the gas turbine maps, temperature leaving the compressor is governed by (2).

$$\Delta T_{comp} = \frac{T_{in,comp}}{\eta_{comp}} \left( \left( \frac{p_{out,comp}}{p_{in,comp}} \right)^{k-1/k} - 1 \right) \quad (2)$$

Similarly, the efficiency equation is adopted to compute the delta in temperature in the turbine [25]. Combustors can be represented in a simplified way, by considering a heat balance around them:

$$\Delta T_{comb} = \frac{LHV}{c_{p,exh} \cdot n \cdot a_t} \quad (3)$$

Equation 3 involves LHV of adopted fuel and theoretical air  $a_t$  for combustion as well as a coefficient  $n$  that consider the real air supplied to the combustion chamber. Heat exchangers are modeled considering the approach proposed in [20] and validated in [21-22]. This is Eq.4.

$$\Delta T_{app} = \Delta T_{app,d} \cdot \left( \frac{\dot{m}_{evolving}}{\dot{m}_{evolving,d}} \right)^\alpha \quad (4)$$

This equation describes the approach temperature difference on the basis of flow evolving through the HX. Ones of the data-driven relations that compose the model is represented by the set of equations (5). Others describe pressure losses, valves characterization etc.

$$\begin{aligned} \dot{m}_{valve} &= f(FO) \\ \Delta p_{loss} &= f(\dot{m}_{flow}) \end{aligned} \quad (5)$$

In the proposed approach, fuel cell stack is modeled with a black-box approach. Temperature of fuel cell has dependence from a wide variety of parameters. Though, at macroscopic level, variation in temperature are driven by energy balance around the stack itself i.e. fuel flow, air flow, current (6).

$$\frac{\Delta T}{T} \propto \sum \frac{\Delta \dot{Q}}{\dot{Q}} = \frac{\Delta \dot{Q}_{fuel}}{\dot{Q}_{fuel}} - \frac{\Delta \dot{Q}_{air}}{\dot{Q}_{air}} - \alpha \frac{\Delta I}{I} \quad (6)$$

Nevertheless, this relationship can be at first simplified by not considering the fuel dependent term: in case fuel utilization is constant, fuel variation is proportional to current. The factor  $\alpha$  is derived from empirical considerations that are based on field data of the plant. No specific operations (e.g. step responses) are requested for parameter identification. Fuel utilization needs to be accurately predicted, as it impacts on both fuel cell voltage and amount of fuel that flows out of the FC stack.  $U_f$  is proportional to the ratio between current and fuel mass flow. In case the amount of hydrogen entering the anode side varies from reference condition,  $U_f$  changes as well. Therefore the formula (7) is proposed, where exponent  $a$  is used for off-design data fitting – consistently with what has been previously presented [20-23].

$$U_f(t) \propto U_f \cdot \left( \frac{H_{2,d}}{H_2} \right)^a \quad (7)$$

Power coming from the cell is computed considering the voltage – since current is an input to the model – as a function of current and air flow, which is driven by thermal load of the cell itself (8).

$$V = V_d \cdot \left( \frac{\dot{m}_{evolving}}{\dot{m}_{evolving,d}} \right)^a \cdot \left( \frac{I_d}{I} \right)^b \quad (8)$$

Again,  $a$  and  $b$  represent off-design parameters that are derived from empirical data identification. Pressure and thermal losses are identified throughout training of the systems based on data plant. These are then implemented in the form of load variations (9).

$$\Delta p_{loss}, \Delta T_{loss} = f(\dot{m}_{evolving}) \quad (9)$$

The numerical part of the model helps to reduce number of states and so complexity and computational effort, though it requires data from plant to train and tune the model. Nevertheless, this is focused on single components and each of them must be trained independently from the others – which improve flexibility of the model itself. Moreover, the accuracy of several parameters is directly dependent from other values. An example is given by Eq. 4 and 5, where evaluation of parameters is directly linked to air mass flow evolution. Furthermore, the complexity and a wide distribution of the data set throughout plant operations is convenient to build a decent numerical structure. For example, it is important to consider at least 10°C of variation of ambient temperature for the data adopted for the training: in this way the identification captures a mid-line of the plant characteristics in everyday working operations. Like other numerical-based model, the better is the data set, the better will result the training. Though, complexity of the resulted model won't change as it is strictly linked to the proposed equations.

## VALIDATION PROCESS

The aforementioned framework has been implemented and validated against real field data for three different emulator rigs. These are located at Thermochemical Power Group (TPG) of University of Genoa (UNIGE), Italy; at the Institute for Combustion

$\frac{\Delta T}{T} \propto \sum \frac{\Delta \dot{Q}}{\dot{Q}} = \frac{\Delta \dot{Q}_{fuel}}{\dot{Q}_{fuel}} - \frac{\Delta \dot{Q}_{air}}{\dot{Q}_{air}} - \alpha \frac{\Delta I}{I}$	$T_{2,ss} = \frac{T_{in,comp}}{\eta_{comp}} \left( \left( \frac{p_2}{p_1} \right)^{k/k-1} - 1 \right)$	$N = f(p_2)$
$U_f(t) \propto U_f \cdot \left( \frac{H_{2,d}}{H_2} \right)^a$	$T_2(t) = T_{2,ss} (1 - e^{-t/\tau})$	$\dot{m}_{valve} = f(FO)$
$\Delta T_{comb} = \left( \frac{LHV_{in}}{c_{p,f} \cdot a_t \cdot n} \right)$	$\tau(t) = \tau_{fl} \left( \frac{\dot{m}_{air}(t)}{\dot{m}_{air,fl}} \right)^a$	$\Delta p = f(\dot{m}_{flow})$
$V = V_d \cdot \left( \frac{\dot{m}_{evolving}}{\dot{m}_{evolving,d}} \right)^a \cdot \left( \frac{I_d}{I} \right)^b$	$\Delta T_{app} = \Delta T_{app,d} \cdot \left( \frac{\dot{m}_{evolving,d}}{\dot{m}_{evolving}} \right)^a$	

Table 1 – Summary of model equations

Technology of German Aerospace Center (DLR) of Stuttgart, Germany; at National Energy Technology Laboratory (NETL) of U.S Department of Energy (DoE) in Morgantown, USA. The three test rigs are intrinsically different each other, and a comparison among the three is not possible. Though, implementation of the approach within these experimental plants is pursued to highlight the capability of obtained models to represent specific dynamic situations of target rig and to outline pros and cons of the approach. Therefore, it resulted in the development and validation of three different models, which however share the same modelling

framework. To enhance accessibility of the tool, results proposed in this work are all derived from implementation of the method within Microsoft Excel/Visual Basic environment. Validation of the model is pursued against real experimental data. The error offered by each model is summarized in a specific table at the end of each paragraph: this includes a percentage error (i.e. the ratio between absolute mean error and nominal value of the parameter) and relative standard deviation (RSD), which gives information about the distribution of the error around the mean value. A threshold of 3% on the error is considered for model validation. Since this work is focused on results of implementation of the model in three different emulator layouts, a brief overview is outlined highlighting the specific features.

### TPG EMULATOR RIG

The first experimental plant targeted for modelling was the emulator rig located at Innovative Energy System Laboratory (IESL) of the Thermochemical Power Group in Savona Campus of the University of Genoa. It is composed by the microturbine manufactured by Turbec – now Ansaldo Energia (AEN) – T100 PHS series 3. The engine has been deeply modified to host a series of pipes, which emulate the cathode and the anode volume in between the compressor and the expander. Globally, the system emulates a 450kW SOFC mGT hybrid system. The test-rig is well described and analyzed in preceding works of the TPG [9], which is here summarized.

The basic generator is able to operate both in stand-alone and grid-connected configurations and it can generate up to 100kW of electrical power. The power unit is composed by a single shaft radial machine revolving at nominal speed of 70000 rpm with a Turbine Inlet Temperature (TIT) of 950°C. The connection with an mGT to an external volume had to be carefully studied: the pressure drop in between the compressor and turbine is the most challenging measurement, which should be minimized to avoid instability, loss in performance and surge.

The equipment included a series of valves that are fundamental for the operations of the engine. These are the vessel bypass valve (VM), which is used to control vessel inlet temperature [8], and the bleed valve (VB), which is used to recover the engine from incoming surge conditions by discharging part of the flow rate in the atmosphere. Pipes that compose the external modular vessel are insulated and are composed of two collector pipes and five modular pipes connected to both collectors, for a maximum volume of 4 m<sup>3</sup> (Figure 1).

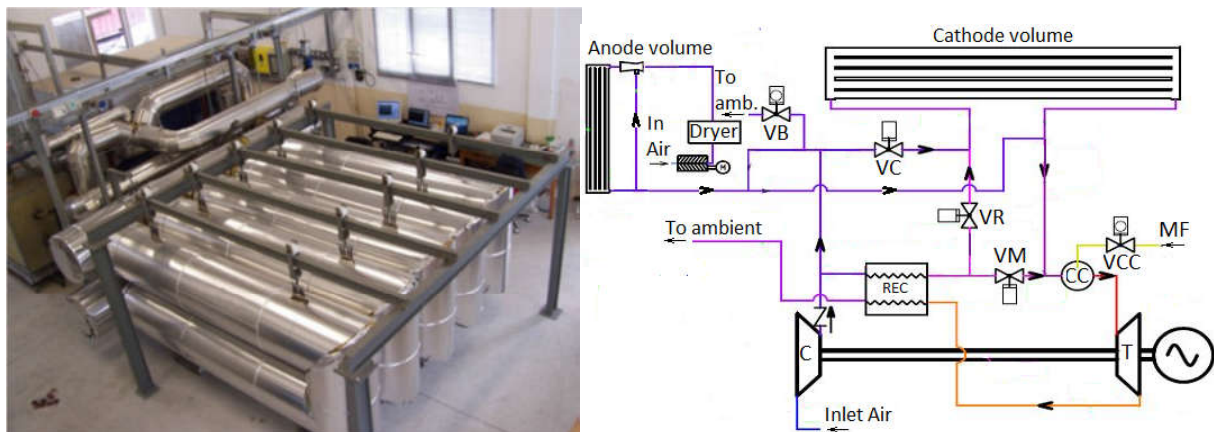


Figure 1 – Reference plant and layout

Thanks to its modular structure, it allows testing of different sized fuel cell stacks. Model01 representing the TPG emulator was the first to be developed and part of the results presented below have been already presented in [23]. The training of the model was based on seven different days of tests and it included the identification of the time constant, which was made considering mechanical and physical characteristics of the plant [23].

Results presented below are obtained grid-connected (GC) configuration for the AEN T100. Model01 was developed with the intent to capture stand-alone configuration as well [23]. Ambient temperature mean value is around 27°C. The test consists on a series of steps in power. These have been chosen to validate the variation in system response in function of evolving flow. At this level, the only input to the model is the compressor outlet pressure (Figure 2). The inputs are constituted by real recorded data, similarly to all the three cases presented. Three variables are shown to compare simulation results against experimental measurements: compressor outlet temperature (COT), generated net power (P), shaft speed (N). Power was increased from 30 kW up to 85 kW through three step changes.

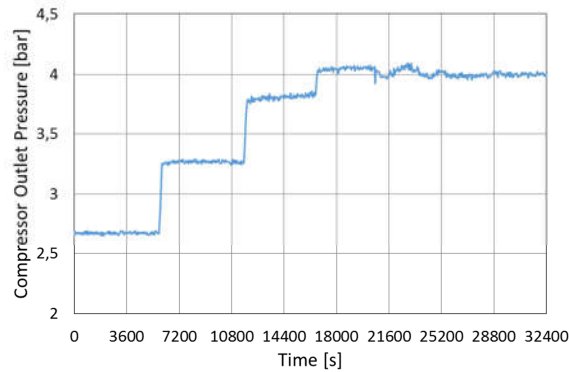


Figure 2 – Input to the model in (a) SA and (b) GC

Figure 3 shows that the model predicted the power output better for lower demands than for higher demands. The shaft speed is presented in Figure 4. This parameter is well reproduced at all load conditions. In this case, the model correctly describes all the variations that occur once the system reaches the full load condition (Figure 4). Nevertheless, the most interesting response is the COT (Figure 5). The COT evolution is strictly linked to turbine maps. When load is increasing the system is pressurizing and air mass flow increases consequently.

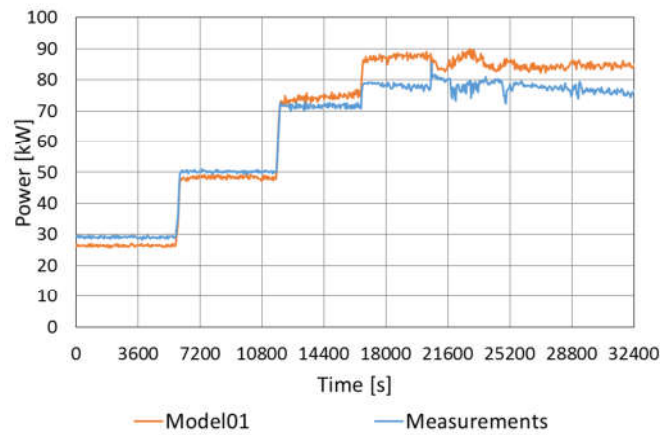


Figure 3 – Power generated in GC configuration

Therefore, time constants of the system are globally higher. Figure 5 shows that the model reproduces COT in GC configuration with some errors in the last steps. Nevertheless, this application shows that implementation of time constant variable on load permits to reproduce load-dependent behaviour of targeted parameters. In conclusion, Table 2 offers a recap of errors computed by the model in simulation process. Average error is expressed in absolute terms. Nominal values are reported for comparison, as well as error percentage and relative standard deviation. In particular it is possible to notice that – considering a threshold of 3% on the error – the power output is the only parameter that overcome this value.

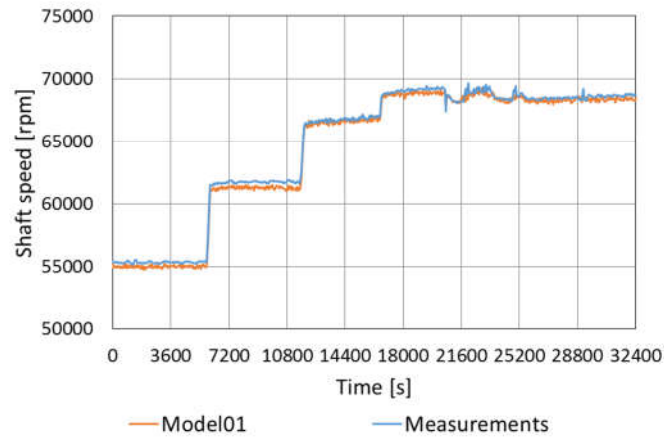


Figure 4 –Shaft speed in GC configuration

	P [kW]	COT [°C]	N [rpm]
MAX	13.3	5.5	467.7
MIN	-5.4	-9.1	-1011
AVG (ABS)	4.6	3.5	288.0
NOMINAL	90	233	70000
PERCENT	5.1	1.5	0.41
RSD	1.0	0.94	0.66

Table 2 – Summary of model errors and nominal values of parameters

It is indeed possible to notice in Table 2 that all the parameters – except the power produced, present a mean error lower than 3% with respect to nominal value. Nevertheless, power generated by the system (which presents a mean error higher than 5%) shows a value for RSD which is similar to the other parameters. Model01 showed to be then sufficiently reliable and presented a set of result consistent for both operating conditions.

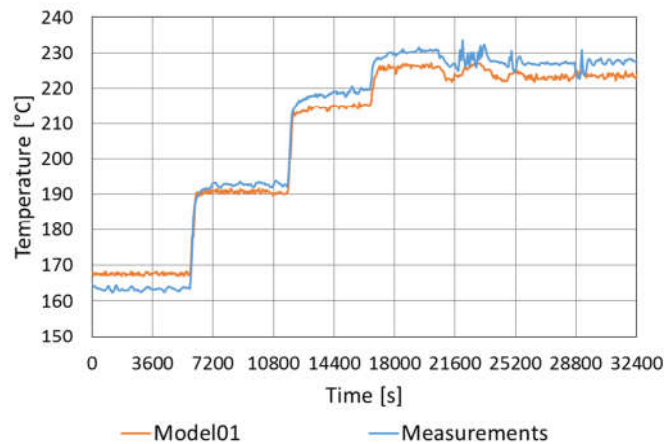


Figure 5 – COT results for GC configuration

## DLR EMULATOR RIG

The second case study was carried out on the German Aerospace Center (DLR) test rig – which drove to development of Model02. In this layout a SOFC emulator is coupled via piping system to the MGT. It is placed in between compressor and turbine. In this plant, the micro GT is the former Turbec T100PH series 3 – the same installed at University of Genoa. The SOFC emulator consists of two pressure vessels. The first one represents the air side volume, with the goal to simulate the impact of a stack of 1152 tubular cells by Siemens [10]. The second pressure volume contains a combustion chamber in order to simulate the thermal release of a fuel cell stack on the evolving flow. Therefore both the thermodynamic and fluid dynamic properties of the SOFC stack can be emulated. It is not possible to emulate the gas composition of the SOFC exhaust gas. The configuration is provided with a so-called hot air path, cold air path and bypass path. These are governed respectively by hot, cold air valve and bypass valve (Figure 6). The hot air and bypass valves regulate the airflow feeding the vessel. A Bleed Air path is connected to the outlet of the compressor to avoid compressor surge. This event occurs when pressure drops in between compressor and turbine are increased. The piping system is connected via special designed interface – a multilayered tubing system – to the turbine. The interface leads the preheated air from the recuperator to the piping system.

The characterization work is still ongoing at DLR. Most recent results have been presented at ASME Turbo Expo 2016 [11]. In this work, the presented model have been applied and implemented to the whole plant, thus validation has been pursued only for those components that have been already undergone a complete characterization process – and so affordable field data were available for validation. With respect to the high amount of data available for the TPG system, in this case only partial operating data have been used for model training.

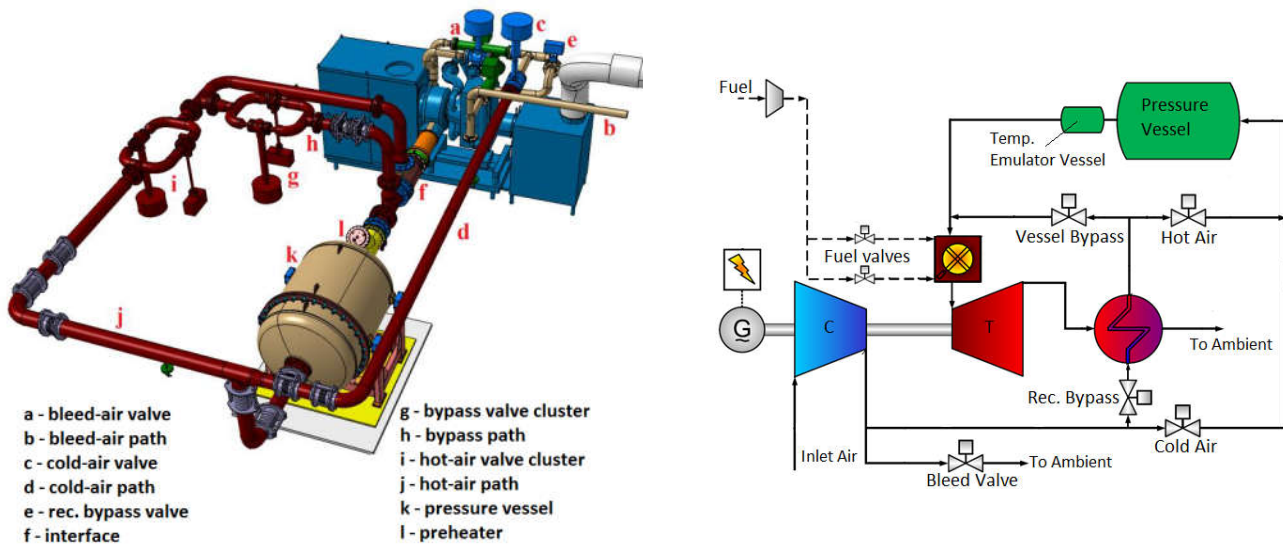


Figure 6 – Reference plant and layout

Therefore, the obtained Model02 was influenced by a tuning based on partially representative recorded data, with consequences on model behaviour. Through this condition, it is possible to deduce how much the training procedure influences the capability of the model to predict the correct behaviour of the system. In this case, two different tests were available for identification of parameters. Model02 was the first to implement valves and pressure and temperature losses throughout the whole systems (this was only partially done in Model01). Thus, inputs to the model were the shaft speed and the valves FO. First results are relative pressure losses and relative temperature losses. The former are calculated as (10), thus considering the global pressure drops in between compressor and turbine. As mentioned before, this is a crucial parameter and it directly influences compressor surge margin. Eq.11 represents temperature drops in between recuperator outlet and vessel outlet.

$$\Delta p_{rel} = \frac{p_{comp_{out}} - p_{turb_{in}}}{p_{comp_{out}}} \quad (10)$$

$$\Delta T_{rel} = \frac{T_{rec_{out}} - T_{vessel_{out}}}{T_{rec_{out}}} \quad (11)$$



Results are presented at steady-state conditions. The orange points belong to model responses, while the blue points represent measured data. In Figure 7 results about relative losses are showed. Results are reported as a function of non-dimensional turbine speed.

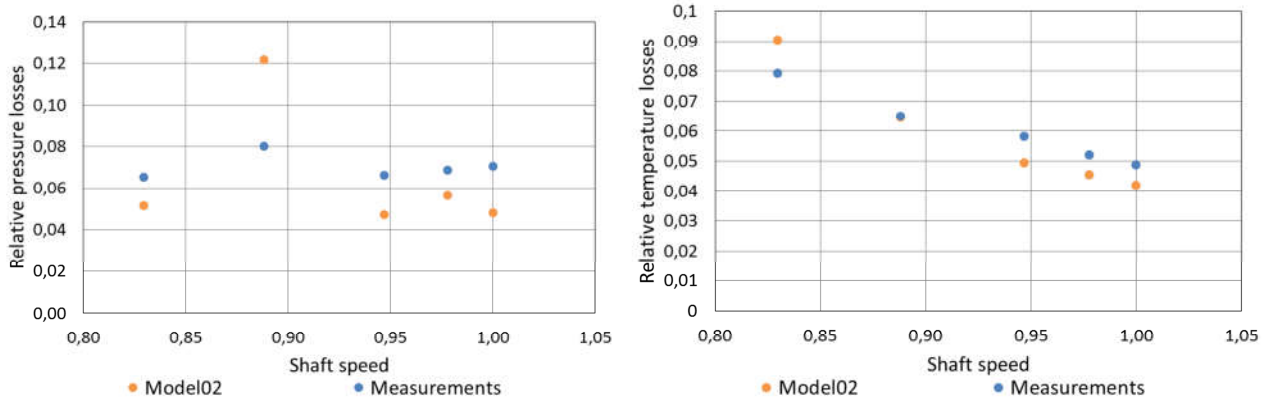


Figure 7 – Relative losses as function of non-dimensional turbine speed

There is an almost constant offset in between what is predicted by the model and what has been measured on the plant (Figure 7). Furthermore, there is also an evident difference in between some points computed by the model with respect to the model trend. Since these two aspects are directly influenced by the system identification process, it is evident in Figure 7 how non-satisfactory can be the response of the model once the training is pursued against a small amount of field data. The recuperator outlet temperature is proposed in Figure 8, while the temperature of the measured points at the vessel outlet is reported in Figure 9. The vessel component is responsible for a temperature drop of 32°C at regime.

Table 4 outlines error measured between model and data. The mean error is evaluated in terms of absolute values.

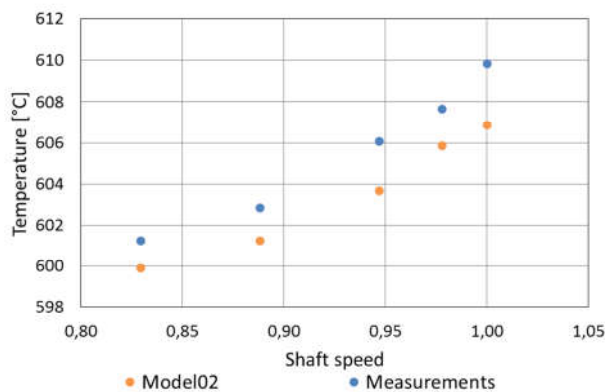


Figure 8 – Recuperator outlet temperatures as a function of shaft speed

In general, the model shows a constant offset in computing these variables. Globally, the model is always shifted from measured results by a certain amount. Since the investigated parameters are derived from equations that are fully trained (Eq.5) or data-driven (Eq. 4), the reduced availability of field data had a negative influence on model precision. Errors emerged also in the first validation proposed (see previous section on TPG test rig), but no constant offset was evident. Considering that steady state conditions should be well reported by the model, the resulting errors can be attributed to the training. Table 3 reports the min, max and average errors in absolute terms with respect to nominal values of investigated variables.

	$\Delta p_{rel}$	$\Delta T_{rel}$	Vessel Out [°C]	Rec Out [°C]
MAX	0.0414	0.0112	5.5	-1.4
MIN	-0.0223	-0.0089	-11	-3.0
AVG (ABS)	0.0218	0.0068	4.9	2.0
NOMINAL	0.0706	0.0487	567	610
PERCENT	30	14	0.86	0.62
RSD	1.21	0.92	1.35	0.33

Table 3 – Summary of model errors together with nominal values of each parameters

The high relative error of the pressure and temperature losses would be not acceptable in a real application. Even though the mean error of the other parameters is good as well as the distribution of the error around the mean value (RSD), the offset that has been showed by the Figures 7-9 is not acceptable. Model02 showed then the influence that the training process has on the simulation results.

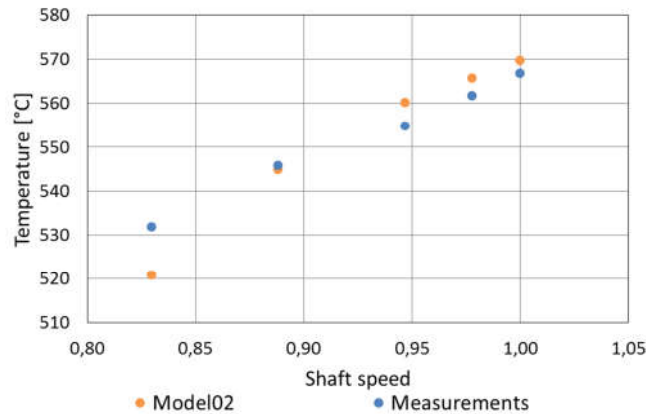


Figure 9 – Vessel outlet temperatures as a function of turbine speed

## NETL TEST RIG

The last implementation was pursued on the NETL HyPer facility test rig. This is based on a SOFC/GT Hybrid System cycle. Similarly to DLR test rig, two pressurized vessels are interposed in between compressor and turbine: the first one simulates the residence time of the cathode side and the second one aims to emulate the heat release of the cell stack. The engine is a 120kW Garrett Series 85 revolving at 40.500 rpm, equipped with a two-stage radial compressor (Figure 10). Two identical counter flow heat exchangers are placed at the outlet of the compressor and recuperate heat from the exhaust flow coming from the turbine. A real-time model is used to compute dynamically the thermal effluent from the stack installed right before the expander. In this case, the coupling of the fuel cell cyber system to the GT physical one is pursued based on the heat released by the stack, which drives the combustor and simulates, in this way, the thermal impact of the stack on the engine. In this layout, three parallel flow paths can be outlined: the bleed air, the cold air and the hot air. These have the same nomenclature of the DLR system; though, they represent slightly different arrangement. Bleed air discharges air flow in the atmosphere directly from the compressor; the cold air path drives the flow from the outlet of the compressor to the inlet of the post combustor volume; the hot air path drives the air flow from the outlet of the recuperator to the post combustor volume. It has been observed that the cold air bypass is very useful to avoid or to recover compressor surge, while the hot air has a lower impact. The HA valve can be used to govern the incoming flow to the cathode. The HyPer facility is designed to simulate the heat release of the SOFC, with a real-time SOFC model to drive the system. As shown in Figure 10b, the real time model is fed with cathode airflow, temperature, and pressure coming from the compressor, in addition with stack load and recirculation condition [5]. Moreover, no manufacturer controller is included in the facility, but controllers are all developed by NETL, and the system can run both in open-loop and closed-loop situations. Currently, this makes the HyPer facility the closest to a real SOFC/GT cycle among the investigated emulators, in terms of dynamic behaviour fidelity.

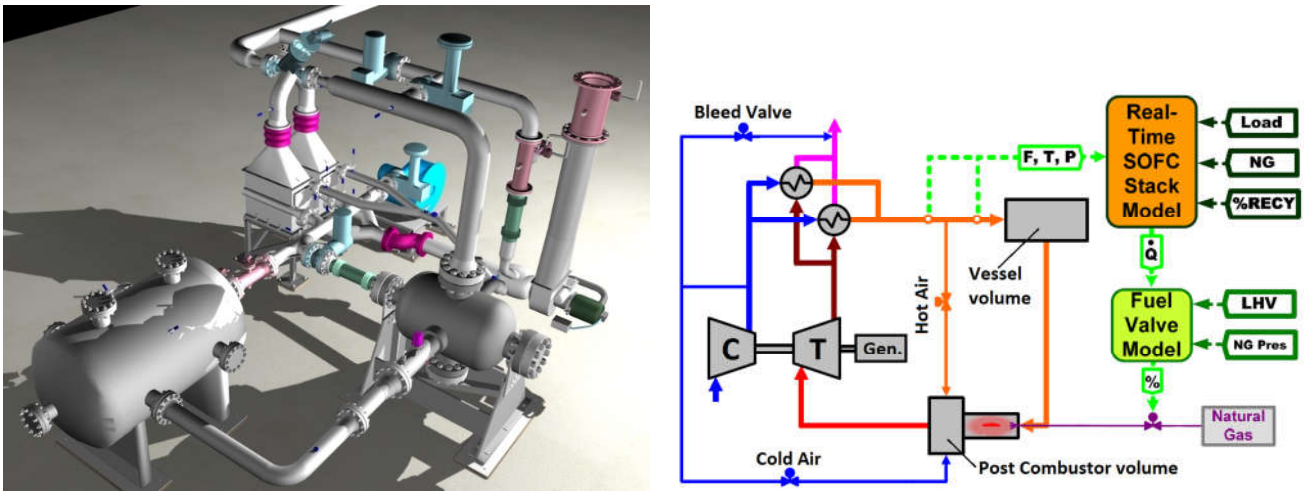


Figure 10 – Reference plant and layout

Implementation of the investigated modelling framework has been accomplished with a particular focus on the fuel cell stack description and validation. In particular, eight different tests conducted at NETL have been used to characterize the system. This is true also for the stack, which was considered a real component to be modelled. Model03 was finally obtained and it was the first one capable to represent a SOFC/GT real system (if compared to Model01 and Model02). The empirical parameter introduced in equation (6) was evaluated through experimental data available, as well as all the off-design exponents introduced in the other equations (Eq.4, 7 and 8). Hereby, one experimental validation of the model for the proposed approach is discussed. In this case, a sequence of steps in FO of CA valve is applied to the system (Figure 11). As stated previously, cold air valve has a great importance in controlling the system, in particular for surge recovery operations. Thus, its influence on system must be accurately captured by the model. Current load to the cell was maintained constant at 220 A for the whole test. Even if variables like current or voltage or stack temperature are addressed as “Measurements” in the results, these are derived from the real-time model in the loop of the hardware installed at NETL facility.

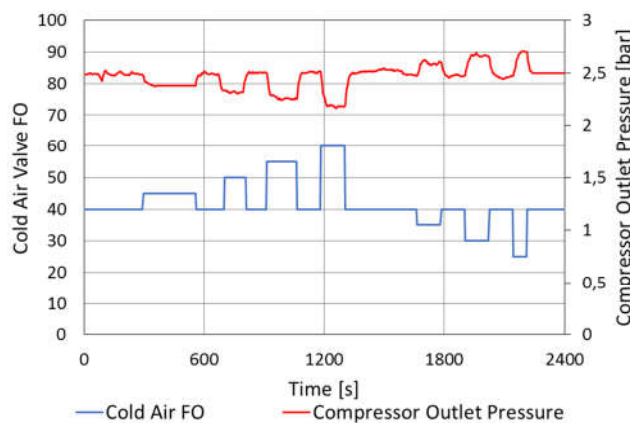


Figure 11 – Input to the model for a cold air steps series

This has been done because they represent the reference target of the presented modelling process. The results presented for Model03 start with considering temperature leaving the recuperator and airflow entering the vessel (Figure 12).

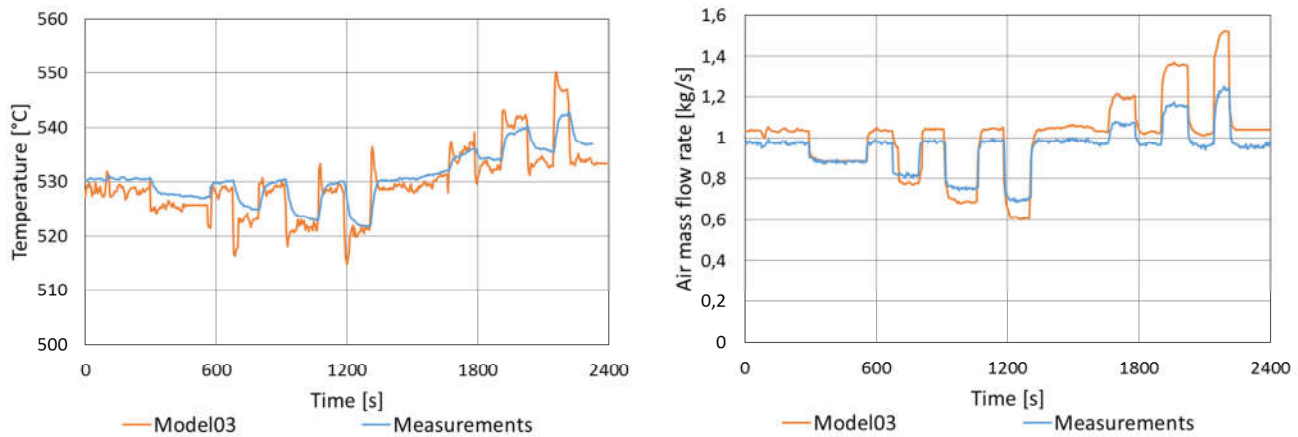


Figure 12 – (a) Recuperator outlet temperature and (b) air mass flow incoming to the vessel.

The high noise level of temperature is due to some amplification gains that are included in temperature computation and linked to mass flow computation. Regardless, the trend is well described for the whole test. Within the vessel system, gas temperature leaving the stack and average temperature of the solid of the stack are shown (Figure 13). Temperature of the solid is described with a first order delay of the gas temperature that leaves the stack – which is the most relevant forcing term for the whole plant (it directly drives the turbine combustor).

The resulting path is then multiplied by a thermal scalar factor, which consider the amount of heat that is exchanged in between stack and airflow as a function of load. Indeed, the temperature of the gas that leaves the fuel cell stack is the results of all time-dependent processes occurring in the stack itself, including at the electrochemical activity. The solid of the stack is influenced in the same way, affected by the high thermal capacitance. Figure 13 shows the gas temperature at the fuel cell stack exit (Figure 13a) and the solid average temperature (Figure 13b).

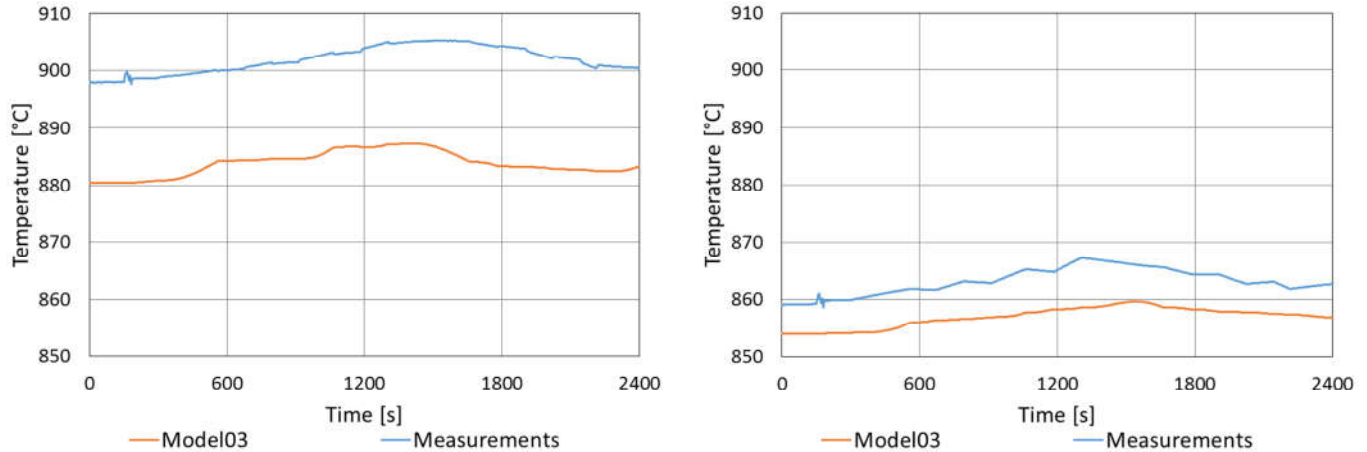


Figure 13 – (a) Temperature of the gas leaving the stack and (b) solid average temperature

Both of them present an almost constant offset. Nevertheless, the error of the model in predicting the temperature of the solid is lower than 1%. In Table 4, simulation errors are summarized. Finally, two other parameters of interest are described in Figure 14: stack voltage and the fuel utilization. In the case of the fuel utilization (Figure 14b), it is possible to notice that cold air variation has an almost negligible influence. On the other hand, cell voltage, reported in Figure 14a, is affected by valve operation, and it shows a small constant offset along the whole test.

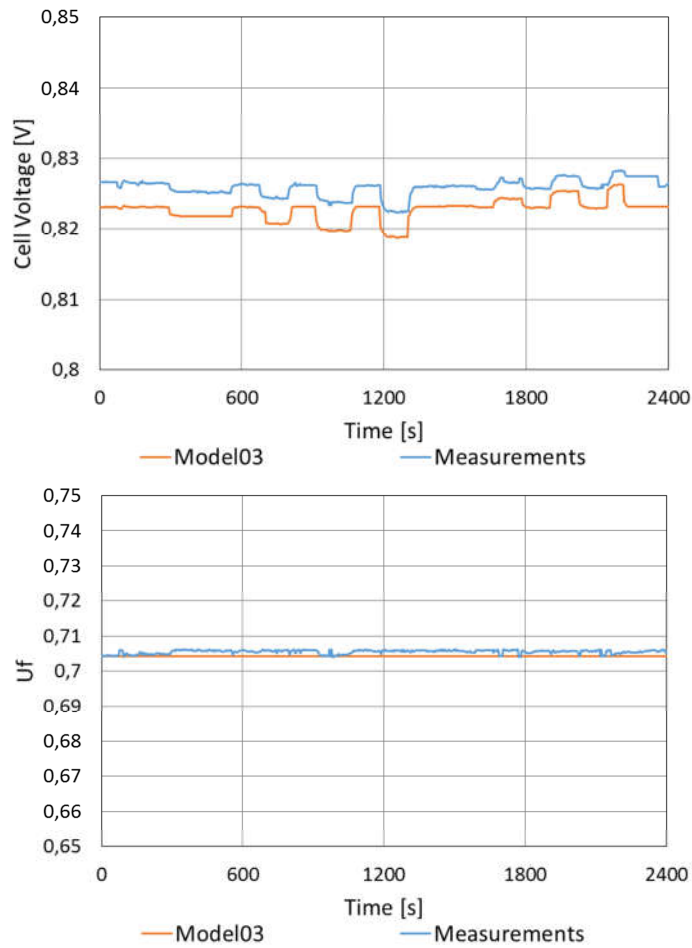


Figure 14 – (a) Cell voltage and (b) fuel utilization factor

It is of interest to analyse in detail the results obtained from Model03. Indeed, these are very similar to what obtained by Model01. One parameter (mass flow in this case) presents a relative mean error which is higher than the adopted threshold, though its RSD is very low – this means the model output is consistent. Besides that, all the other parameters are well represented by the model: both error and RSD are limited. Again, considering a sufficient variety of data used for the training, the model offers a reliable and consistent response. Thus, Model03 showed the feasibility of the approach for the stack – and so for the whole system

	T air leaving recuperator [°C]	Air flow to the vessel [kg/s]	T gas leaving stack [°C]	T solid average [°C]	Voltage [V]	Uf
MAX	12.2	0.32	-15.7	-4.4	-0.0006	0.0002
MIN	-13.1	-0.20	-21.0	-8.6	-0.0053	-0.0019
AVG (ABS)	2.47	0.08	18.0	6.2	0.0031	0.0012
NOMINAL	530	0.97	897	859	0.83	0.7
PERCENT	0.47	8.2	2.0	0.72	0.37	0.17
RSD	1.01	0.14	0.07	0.21	0.43	0.08

Table 4 – Summary of model errors and nominal values of each considered parameters

## CONCLUSIONS

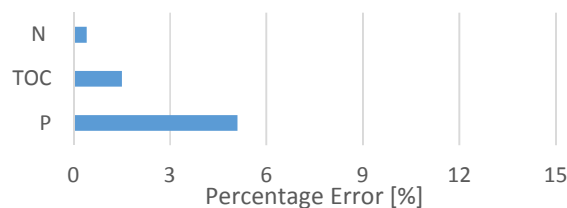
An innovative approach to model a SOFC/GT hybrid power plant has been developed and validated against three different test-rig layouts installed respectively in Italy (TPG), Germany (DLR) and USA (NETL). The same framework has been then applied to three different plant without significant changes and considering a rapid training to tune part of the models properly. This drove to development of three different models, which aim to a dynamic description of the target system. The trio is based on the same modelling framework, which is composed both by physical principles and data training. Results presented are obtained through implementation on Microsoft Excel/Visual Basic environment.

Such framework is able to provide a model with a minimal computational time: all the models used less than one minute to compute the results proposed in this work on a traditional desktop PC. For sure, the resulting accuracy of predictions is far from high granularity models, but the application field is completely different. The training process is fundamental to enhance the precision of the model, but this come with the limitations of data-driven model: need for data, identification process. Nevertheless, since the training is conducted *per component*, it is not necessary to perform a brand new system identification in case one element (e.g. a valve) is changed in the real plant. Furthermore, the training of the system is performed through normal operating data and there is no need to drive the target system to accomplish specific operations (such as step responses) to favour the identification of the system. After the application of such modelling approach to three different emulator rigs, the following conclusions can be drawn:

- Dynamic modelling through time constants for non-linear systems needs to be strongly correlated to evolution of constants themselves during the operations of the plant. Load-dependent time constants have been introduced and their effect was clearly visible in the validation of the model pursued at TPG.
- The numerical basis of the approach is of strong importance to reduce computational efforts and simplify representation of the final plant. In fact, the model can be tuned basing on recorded data derived from normal operating conditions of the plant. However, if seven different operations were enough to accurately represent both TPG and NETL rigs, the two used for the DLR were not sufficient.
- The approach was globally validated at NETL on the cyber-physical facility. For a stressing load situation derived by a series of steps in the cold air valve regulation, the model responded in fairly accurate manner and, even if a final offset was present, the temperature of the fuel cell solid was captured by the model with an average error of 6°C in absolute terms.

Even though the three models have been trained through different data sets (in terms of amount of measurements available), it can be stated that seven days of operations can suffice to give a first affordable characterization of the system. Indeed, a comparison of results between Model01 and Model03 shows that with a consistent data set available for the training, the response of the model is in general reliable. Importance of system identification is even more evident for Model02. There, for those parameters that only depend from this procedure, the error was too high. For the others parameters, an offset was always present in the results. Considering the RSD, the three models showed a good consistency in the three tests: globally they range around 1, which means a low scattering of the simulation results. Figure 15 gives a summary of validation of the models. Considering the aforementioned threshold of 3%, it is possible to notice that:

- In Model01 the highest error was related to power output prediction (close to 6% in both configuration).
- In Model02 the low availability for data for the training shows a strong influence on relative pressure and temperature drops – i.e. those parameters that are directly derived from system identification. In this case the maximum average error was around 30% (with a consistent offset from the field data adopted for validation, see Figure 7a).
- Model03 showed a behaviour similar to Model01: with comparable amount of data available for the training, it resulted the temperature of air incoming the vessel the only parameter above the 3%



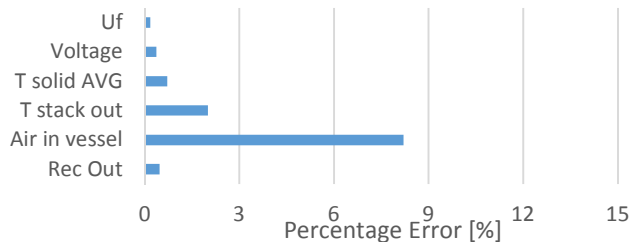
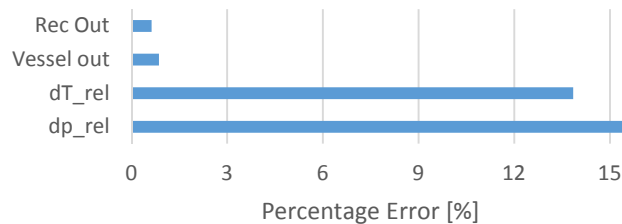


Figure 15 – Errors recap of the three models, starting from Model01 down to Model03

After validation of this simplified physics-based approach to dynamic modelling of energy systems, now such a model can be exploited for advanced control system development. In fact, such models can now be used to build model-based controllers with a reduced number of states or to define dynamic physics-based observers for fuel cell parameters not directly measurable, starting from available measurements such as air mass flow, electrical current and system temperatures. In particular, such framework can open new ways for model-based controllers application [24].

#### DISCLAIMER

This report was prepared as an account of work sponsored by an agency of the United States Government. Neither the United States Government nor any agency thereof, nor any of their employees, makes any warranty, express or implied, or assumes any legal liability or responsibility for the accuracy, completeness, or usefulness of any information, apparatus, product, or process disclosed, or represents that its use would not infringe privately owned rights. Reference therein to any specific commercial product, process, or service by trade name, trademark, manufacturer, or otherwise does not necessarily constitute or imply its endorsement, recommendation, or favoring by the United States Government or any agency thereof. The views and opinions of authors expressed therein do not necessarily state or reflect those of the United States Government or any agency thereof.

#### NOMENCLATURE

##### Acronyms

CA	= Cold Air valve
CFD	= Computational fluid dynamics
COT	= Compressor outlet temperature
DLR	= German Aerospace Center
DoE	= Department of Energy
FO	= Fractional Opening
GT	= Gas Turbine
HA	= Hot Air valve
HS	= Hybrid System
HX	= Heat Exchanger
IESL	= Innovative Energy System Laboratory
NETL	= National Energy Technology Laboratory
P	= Power output
RSD	= Relative Standard Deviation
SOFC	= Solid oxide fuel cell
TOT	= Turbine outlet temperature



TIT = Turbine inlet temperature  
 TPG = Thermochemical Power Group  
 UNIGE = University of Genoa

### Parameters

$\eta$  = efficiency  
 $\tau$  = time constant [s]  
 $H_2$  = hydrogen concentration [mol/m<sup>3</sup>]  
 $h_i$  = i-th specific enthalpy [kJ/kg]  
 $I$  = current [A]  
 $\dot{m}_i$  = i-th mass flow [kg/s]  
 $N$  = shaft speed [rpm]  
 $p$  = pressure [bar]  
 $\dot{Q}_i$  = i-th heat flux [kW]  
 $T_i$  = i-th temperature [K]  
 $U_f$  = Fuel utilization  
 $V$  = Voltage [V]

### Subscripts

*a* = off-design parameter  
*app* = approach difference  
*comb* = combustor parameter  
*comp* = compressor parameter  
*d* = design parameter  
*in* = into control volume  
*normalized* = normalized parameter  
*out* = out of control volume  
*shaft* = shaft parameter  
*ss* = steady state  
*turb* = turbine parameter

### REFERENCES

- [1] "Distributed Fuel Cell - Energy Recovery Generator (DFC-ERG) by FuelCell Energy" [www.fuelcellenergy.com](http://www.fuelcellenergy.com), last access 29/09/2016
- [2] Kabata T., Nishiura M., Tomida K., Koga S., Mataka N., 2008, Fuel cell seminar & exposition 2008. pp. 263-267.
- [3] Mitsubishi Heavy Industries, 2015, "Demonstration of SOFC-Micro Gas Turbine Hybrid Systems for Commercialization", Mitsubishi Heavy Industries Technical Review, vol. 52 (4) .
- [4] Owens B., McGuinness J., 2015, "GE-Fuel Cells: the power of tomorrow", [www.ge.com](http://www.ge.com), last access 20/11/2016
- [5] Zaccaria V., Tucker D., Traverso A., 2016, "Transfer function development for SOFC/GT hybrid systems control using cold air bypass", Applied Energy vol. 165, pp. 695-706.
- [6] Tucker D., Lawson L., Gemmen R., 2003, "Preliminary Results of a Cold Flow Test in a Fuel Cell Gas Turbine Hybrid Simulation Facility", ASME paper GT-2003-38460.
- [7] Ferrari M. L., 2015, "Advanced control approach for hybrid systems based on solid oxide fuel cells", Applied Energy, vol. 145, pp 364-373.
- [8] Larosa L., Traverso A., Ferrari M. L., and Zaccaria V., 2014, "Pressurized SOFC Hybrid Systems: Control System Study and Experimental Verification," Journal of Engineering for Gas Turbines and Power, vol. 137(3), p. 31602.
- [9] Ferrari M.L., Pascenti M., Bertone R., Magistri L., 2009, "Hybrid simulation facility based on commercial 100kWe Micro Gas Turbine", Journal of Fuel Cell Science Technology, vol.6
- [10] Hohloch M., Huber A., Aigner M., 2014, "Experimental investigation of a SOFC/MGT Hybrid Power Plant test rig - Impact and characterization of coupling elements", ASME Turbo Expo 2014, Dusseldorf, Germany, GT2014-25918
- [11] Hohloch M., Huber A., Aigner M., 2016, "Experimental investigation of a SOFC/MGT Hybrid Power Plant test rig - Impact and characterization of a fuel cell emulator", ASME Turbo Expo 2016, Seoul, South Korea, GT2016-57747
- [12] Wang K., Hissel D., Péra M.C., Steiner N., Marra D., Sorrentino M., Pianese C., Monteverde M., Cardone P., Saarinen J., 2011, "A review on solid oxide fuel cell models", International journal of hydrogen energy, vol. 36, pp. 7212-7228.



- [13] Kim S., Pilidis P., and Yin J., 2000, "Gas Turbine Dynamic Simulation Using Simulink®", Power Systems Conference, San Diego.
- [14] Roberts R., Brouwer J., Jabbari F., Junker T., 2006, Hossein Ghezeli-Ayagh, "Control design of an atmospheric solid oxide fuel cell/gas turbine hybrid system: Variable versus fixed speed gas turbine operation", *Journal of Power Sources*, vol. 161, pp. 484-491.
- [15] Ferrari M. L., Traverso A., Massardo A. F., 2004, "Transient Analysis of Solid Oxide Fuel Cell Hybrids. Part B: Anode Recirculation Model", ASME Turbo Expo 2004, Vienna, Austria, GT2004-53716.
- [16] Ferrari M.L., Magistri L., Traverso A., Massardo A. F., 2005, "Control System for Solid Oxide Fuel Cell Hybrid Systems", ASME Turbo Expo 2005, Reno, Nevada, GT2005-68102.
- [17] Traverso A., Trasino F., Magistri L., Massardo A.F., 2008, "Time characterisation of the anodic loop of a pressurized solid oxide fuel cell system", *Journal of Engineering for Gas Turbines and Power*, vol. 130, 021702-1/9.
- [18] Wächter C., Fraqnz Joos R.L., 2006, "Dynamic Model of a Pressurized SOFC/Gas Turbine Hybrid Power Plant for the Development of Control Concepts", *Journal of Fuel Cell Science and Technology*, vol.3, pp. 271-279.
- [19] Henke M., Monz T., Aigner M., 2016, "Introduction of a new numerical simulation tool to analyze micro gas turbine cycle dynamics", *Journal of Engineering for Gas Turbine and Power*, vol.139(4).
- [20] Gulen S.C., Kim K., 2013, "Gas Turbine combined cycle dynamic simulation: a physics based simple approach", ASME Turbo Expo 2013, Montreal, Canada. GT2013-94584
- [21] Rossi I., Sorce A., Traverso A., Pascucci F., 2015, "A simplified hybrid approach to dynamic model a real HRSG", ASME Turbo Expo 2015, Montreal, Canada, GT2015-42654
- [22] Rossi I., Sorce A., Traverso A., 2017, " Gas turbine combined cycle start-up and stress evaluation: A simplified dynamic approach" , *Applied Energy*, vol. 190, pp. 880-890
- [23] Roberts R., Rossi I., Traverso A., 2015, "Dynamic simulation of energy systems: comparison of a physics-based against time constant based approach applied to a microturbine test rig" , ASME Turbo Expo 2015, Montreal, Canada, GT2015-42651.
- [24] Rossi I., Zaccaria V., Traverso A., 2017, "Advanced control for cluster of SOFC/GT Hybrid Systems", ASME Turbo Expo 2017, Charlotte, USA, GT2017-64194.
- [25] Cohen H., Rogers G.F.C., Saravanamuttoo H.I.H., 1996, "Gas Turbine Theory" 4<sup>th</sup> edition Lomgman Group